

## Towards modelling bloodstain formation

M. Sellier<sup>1</sup>, G. Baechtel<sup>2</sup> and M.C. Taylor<sup>3</sup>

<sup>1</sup>Department of Mechanical Engineering  
 University of Canterbury, Private Bag 4800, Christchurch 8140, New Zealand

<sup>2</sup>ESSTIN  
 2, Rue Jean Lamour, Vandoeuvre les Nancy Cedex, F 54519, France

<sup>3</sup>Institute of Environmental Science and Research  
 27 Creyke Rd, Christchurch 8031, New Zealand

### Abstract

The work presented here is a first attempt to model the impact of blood droplet in the view of understanding and predicting bloodstain formation to help forensic scientists in their endeavour against crimes. We have tried here to model the droplet impact using the commercial Computational Fluid Dynamics software Fluent<sup>TM</sup>. In parallel, we have used high-speed imaging to track blood droplet impacts. Two sets of results are reported here for which the Weber number is 240 and 419 and the Reynolds number is 1970 and 1420. In this parameter range the droplet does not splash upon impact. The maximum spread radius obtained numerically is found to be within 15% of the one obtained experimentally. This result is deemed encouraging because of the approximations made.

### Motivation

Bloodstain pattern analysis (BPA) is an important pre-requisite to the understanding of blood shedding events. The examination of the shape and distribution of bloodstains can sometimes provide valuable information for crime scene investigators. One of the important pieces of information which may be inferred from impact spatter patterns is the area of origin of the spatter. It is deduced from the knowledge of the position of bloodstains in the pattern, their directionality, their impact angles, and elementary trigonometry. The impact angle of blood droplets can be determined with the celebrated "sine formula" which states that the ratio of the minor to major axis lengths of an ellipse fitted through the bloodstain is equal to the sine of the angle of impact i.e.,  $\sin \theta = W/L$  as shown in Figure 1.

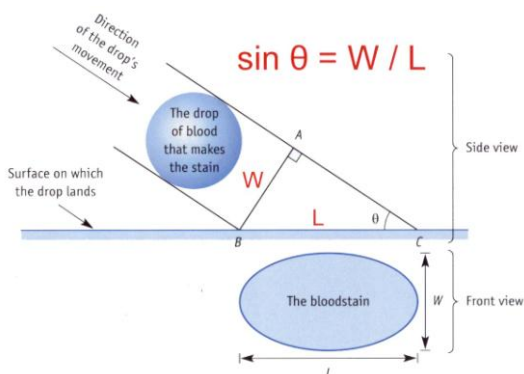


Figure 1. This figure illustrates the classical view on the origin of the sine formula

The textbook justification for the sine law is that the bloodstain footprint is essentially the projection of the blood droplet in flight on the solid surface, as illustrated in Figure 1. This remarkably

simple law has shortcomings and limitations and in order to understand its origin and range of applicability, a deeper analysis of the fluid mechanics involved is needed. The impact of a droplet on a solid surface is a classical fluid dynamics problem but very little has been done in the context of blood. The work presented here, a first step in this direction, is a combined numerical and experimental study of the normal impact of blood droplets on smooth surfaces. The next section summarizes well known facts on droplet impacts and the particularity of blood as a fluid. This section is followed by a section describing the acquisition of blood droplet impact data and the CFD model. Finally, experimental and numerical results are compared and discussed.

### Background

The impact of droplets has been intensively studied over the past because of its prevalence in the number of industrial applications such as inkjet printing or spray coating but also because it encompasses some of the most difficult modelling challenges in fluid mechanics such as a free surface, a wetting front, or topology changes. As the droplet impacts on the solid surface the kinetic energy of the droplet is transformed into surface energy (potential energy) and dissipated by viscous shear. A simple dimensional analysis reveals that the main dimensionless terms relevant to the impact dynamics are the Reynolds number

$$Re = \rho D V_0 / \mu \text{ and Weber number } We = \rho D V_0^2 / \sigma,$$

where  $\rho$ ,  $\sigma$ , and  $\mu$  are the density, surface tension, and dynamic viscosity of the droplet of diameter  $D$  impacting with the velocity  $V_0$ , [5]. The first dimensionless term expresses the ratio of inertia to viscous forces and the second that of inertia to surface tension. Another dimensionless number commonly used in the description of droplet impact is the Ohnesorge number which is a combination of the Reynolds and Weber numbers defined as

$$Oh = We^{1/2} Re^{-1}.$$

Rioboo and co-workers give 6 possible outcomes of the droplets impacts: deposition, prompt splash, corona splash, receding break-up, partial rebound, and complete rebound, [3]. The regime of interest here is the deposition regime for which no apparent splashing occurs. Mundo et al. introduced a splashing parameter defined as  $K_d = We^{1/2} Re^{1/4}$  and found that for the set of results they considered, splashing occurs when  $K_d > 57.7$ , [2]. A quantity of major importance in the

present study is the maximum spread radius since it is related to the final bloodstain appearance. Scheller and Bousfield proposed the following empirical correlation for the maximum spread radius of droplets of Newtonian fluids [4]:

$$\xi = 2R_{\max}/D = 0.61(\text{Re}^2 \text{Oh})^{0.166} \quad (1)$$

Unsurprisingly, most of the existing results pertain to Newtonian fluids but blood is a suspension of red blood cells, white blood cells and platelets in a plasma made of gases, salts, proteins, carbohydrates, and lipids. By volume the red blood cells constitute about 45% of whole blood, the plasma constitutes about 55%, and white blood cells constitute a minute volume. Whole blood (plasma and cells) exhibits a non-Newtonian rheology, i.e. the apparent blood viscosity depends on the shear rate. At low shear rates, rouleaux formation and sedimentation lead to a high apparent viscosity whilst at high shear rate, the stacks break down resulting in a Newtonian behaviour. Another feature of blood rheology is that a yield stress exists, i.e. flow can only occur if the shear rate exceeds a given threshold. For the modelling part of this preliminary study, the blood will be assumed to be Newtonian with the following properties:  $\rho=1062 \text{ kg/m}^3$ ,  $\mu=4.75 \times 10^{-3} \text{ Pa}\cdot\text{s}$ ,  $\sigma=5.55 \times 10^{-3} \text{ N/m}$  which are typical values.

### Data acquisition

Blood droplets were released from a pipette positioned at a given height above a substrate. The droplet free fell and impacted on a smooth surface (either glass or Perspex). The impact was recorded using a high-speed camera at a rate of up to 5,000 fps. The impact velocity of the droplet was inferred by straightforward energy conservation argument, i.e. if all the potential energy of the falling droplet is transformed into kinetic energy, we must have  $V_0 = \sqrt{2gh}$ . The following discussion focuses on two sets of results. For **Result Set I**, the droplet was released from 315 mm and impacted on a glass surface and for **Result Set II**, it was released from 200 mm and impacted on a Perspex surface. This corresponds to impact velocities of 2.49 m/s and 1.98 m/s, respectively.

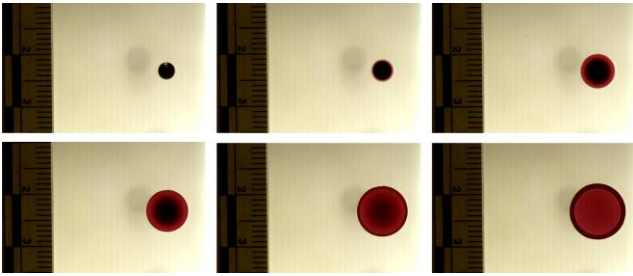


Figure 2. Captured images for the normal impact of a blood droplet on Perspex (**Results Set II**)

Figure 2 illustrates some of the captured images for the impact of a blood droplet on a Perspex surface. The viewpoint is from directly above. The Matlab™ image processing toolbox is used to manipulate the images. Once the image is transformed into a binary image (black and white), a circle is fitted to the outline of the droplet. The following process is used to manipulate the images. Each images' colour map is adjusted to give a photo-negative version of the image. This is to allow the droplet to be white once it is adjusted to a binary image. The photo-negative image is then converted to a binary image with a suitable threshold value to ensure the outline of the droplet is clear and sharp. Next a boundary between the white droplet and the black contour is traced. The co-ordinates of the points that formed the traced outline of the droplet are used to perform a least-squares fit of a circle. The droplet diameter before impact is determined by taking readings of pixels from an image that shows the droplet before impact. The number of pixels of the fitted circle's diameter is scaled by a pixel reading from a line section using the

ruler markings. The droplet diameters are found to be 3.54 mm and 3.2 mm for **Result Set I** and **II**, respectively. The relevant dimensionless groupings are reported in Table 1.

Result Set	$Re$	$We$	$Oh$	$K_d$
<b>I</b>	1970	419	0.0104	136
<b>II</b>	1420	240	0.0109	95

Table 1. Relevant dimensionless groupings.

Another important parameter affecting the impact dynamics is the wettability of the substrate quantified by its static contact angle. The static contact angle is measured with a KSV CAM200 goniometer by depositing a droplet on the substrate, recording the equilibrium droplet shape, and fitting this to the Young–Laplace equation. It is found to be  $53^\circ$  for the glass and  $44^\circ$  for the Perspex.

### CFD modelling

Modelling the impact of droplets has been attempted by many authors and it is beyond the scope of this work to review all the relevant work. The interested reader can refer to [6] for a good review. We use here the commercial CFD package Fluent™ which is a Finite Volume based solver. In spite of the obvious axi-symmetry of the normal impacts, we have used a three-dimensional mesh because oblique impacts will ultimately be modelled and it is therefore advantageous to infer good modelling practice for normal impacts with realistic mesh densities. The computational domain was tessellated with approximately 400,000 cells refined in the expected trajectory of the impacting droplets. Approximately 15 cells per radius of the initial droplet proved to be a good compromise between the computational resource requirements and the solution accuracy.

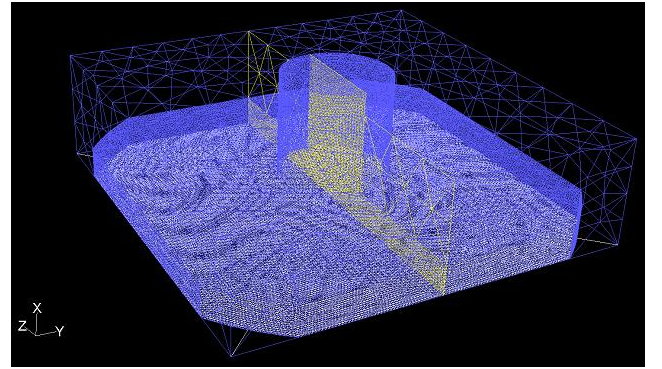


Figure 3. Three-dimensional mesh for modelling the impact dynamics.

Fluent™ uses the Volume Of Fluid (VOF) method which is an Eulerian method to track the interface between the two phases (blood and the surrounding air). In the VOF scheme, a single set of momentum equations is shared by the fluids and the volume fraction of each of the fluids in each computational cell is computed throughout the domain. In each computational cell,  $\alpha_q$  denotes the volume fraction of the  $q^{\text{th}}$  phase such that when  $\alpha_q = 1$ , the cell is saturated with the  $q^{\text{th}}$  phase and when  $\alpha_q = 0$  it is devoid of the  $q^{\text{th}}$  phase. The interface is located in any cell for which this volume fraction is between 0 and 1. In the following, air is the primary phase (subscript 1) and blood is the secondary phase (subscript 2). Fluent™ solves the Navier-Stokes equations in the entire computational domain as

$$\frac{\partial}{\partial t}(\rho) + \nabla \cdot (\rho \vec{v}) = 0 \quad (2)$$

$$\frac{\partial}{\partial t}(\rho \vec{v}) + \nabla \cdot (\rho \vec{v} \vec{v}) = -\nabla P + \nabla \cdot [\mu(\nabla \vec{v} + (\nabla \vec{v})^T)] + \rho \vec{g} + \vec{F}(3)$$

$\vec{v}$  is the velocity vector,  $P$  the pressure,  $\vec{g}$  the acceleration of gravity, and  $\vec{F}$  is the surface tension per unit volume vector force. As we have a two phase problem, the density and viscosity of the mixture are calculated as:

$$\rho = \alpha_2 \rho_2 + (1 - \alpha_2) \rho_1 \quad (4.a)$$

$$\mu = \alpha_2 \mu_2 + (1 - \alpha_2) \mu_1 \quad (4.b)$$

In the VOF method, the motion of a moving interface is computed by solving an advection equation for the volume fraction  $\alpha_2$  of the secondary phase:

$$\frac{\partial}{\partial t} (\alpha_2) + \vec{v} \cdot \nabla \alpha_2 = 0 \quad (5)$$

The volume fraction of the primary phase is then obtained from the following constraint  $\alpha_1 + \alpha_2 = 1$ .

The surface tension model incorporated in Fluent<sup>TM</sup> is the Continuum Surface Force (CSF) model by Brackbill et al., [1]:

$$\vec{F} = \sigma \kappa \frac{\nabla \alpha_2}{\frac{1}{2}(\rho_1 + \rho_2)} \quad (6)$$

where  $\kappa$  is the interface curvature given by:

$$\kappa = -(\nabla \cdot \vec{n}) \quad (7)$$

In order to account for the partial wettability of the substrate, we need to impose a condition at the dynamic contact line. Fluent<sup>TM</sup> allows the user to impose a ‘‘wall adhesion’’ condition whereby the following constraint is imposed at the contact line:

$$\vec{n} = \vec{n}_w \cos \theta + \vec{t}_w \sin \theta \quad (8)$$

where  $\vec{n}_w$  and  $\vec{t}_w$  are the unit vectors normal and tangential to the wall, respectively, and  $\theta$  is the contact angle. Note that we use here the static contact angle ( $53^\circ$  for glass and  $44^\circ$  for Perspex) which is an over-simplification because the observable contact angle is dependent on the contact line velocity. Fluent<sup>TM</sup> does not yet provide the option to parameterize the contact angle with the contact line velocity and one of the objectives of this study is to assess the effect of this restriction.

The following reports the settings used in Fluent:

- The droplet is assumed to be spherical and in free fall. The blood and air are assumed to be Newtonian and incompressible with standard properties for air.
- We use the pressure based Fluent solver and an unsteady formulation with a first order, explicit time discretization scheme. The Implicit Body Force is enabled to help the simulation because of the strong density gradient.
- Gravity is included in the simulations because the Bond number defined as  $Bo = (\rho_2 - \rho_1)gD^2/\sigma$  is greater than 1.
- Time steps of  $10^{-6}$  s lead to successful simulations. At least 20 iterations per time step are used to decrease the residuals to below  $10^{-3}$ .
- The solution is controlled with a PISO Pressure-Velocity coupling and PRESTO discretization for the pressure. First order and geo-reconstruct are used for the momentum and VOF equations, respectively.

The solid surface is modelled as a wall with a no-slip condition and an adhesion constraint set such that the contact angle is  $\theta$ . The other boundaries are set to Pressure Inlet where Pressure and Initial Gauge Pressure is equal to zero for each phase. All variables are initialized to zero. A sphere is then marked on the solution domain where the blood volume fraction is set to one

and the velocity is imposed to be the same as that of the experiments.

## Results

The impact of a blood droplet typically involves four different stages which depend on initial conditions and physical properties:

1. **Contact and collapse:** the droplet contacts the target surface and collapses from bottom up. The part of the drop that has not yet collided with the surface remains as part of the sphere. As the collapse occurs, the blood that has come in contact with the surface is forced outward creating a rim. The rim gets bigger as more of the droplet comes in contact with the surface and more blood is forced into the rim.
2. **Displacement:** in this stage, the blood droplet has collapsed against the target surface and nearly all the blood has moved from the centre of the droplet to the rim. The actual area of displacement will be the same size as the eventual stain. At the edge of the rim will be dimples and short spines. In this stage the movement of the blood is lateral to the sides.
3. **Dispersion:** In this phase, most of the blood is forced to the rim, especially when a high velocity occurs. The spines and dimples continue to rise upward and in a direction opposite to the original momentum. As the amount of blood in the rim and spines increases, they become unstable.
4. **Retraction:** the last phase results from the effect of surface tension attempting to pull back the droplet. If the forces trying to pull the droplet apart are overcome by surface tension, the resulting stain will be reasonably circular and symmetrical in shape. If the force pulling the droplet apart overcomes surface tension, the droplet will burst and create an irregular stain pattern.

Figure 4 shows a sequence of images of the droplet profiles computed at various times.

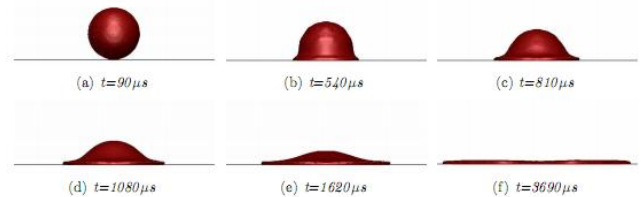


Figure 4. Simulation results at various times for the normal impact on Perspex (**Results Set II**)

The impact starts at  $90 \mu s$ . After impact, the droplet adopts a bell-like shape with a thin liquid layer expanding radially outwards at the base. It takes between 3 and 4 ms for the droplet to reach its maximum spread radius. At that stage the droplet assumes the shape of a flat pancake. The picture sequence illustrates the various stages stated above and is very reminiscent of the prompt splash regime shown in the paper of Rioboo et al., [3]. A more quantitative comparison is shown in Figures 5 where the experimental and computed spread radius (the radius of the footprint of the stain as a function of time) is plotted as a function of time. Note that we use here dimensionless units.

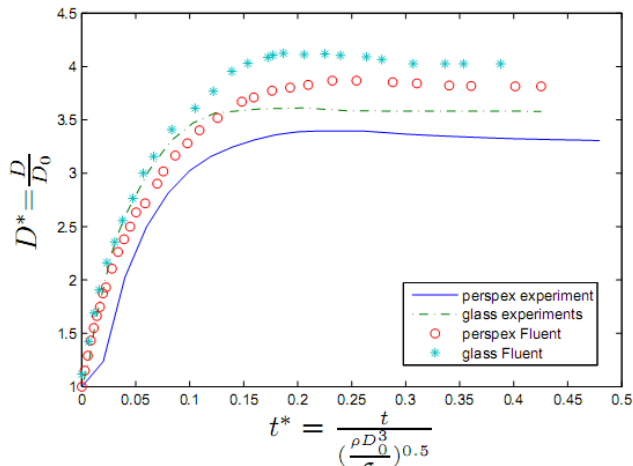


Figure 5. Time variation of the spread radius in dimensionless units.

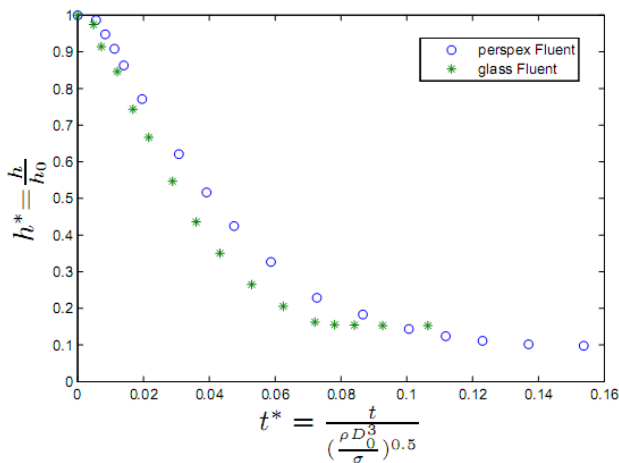


Figure 6. Time variation of the droplet height in dimensionless units.

The numerical and experimental results agree reasonably well. The trend in the spread radius variation is well captured by Fluent and the fact that the final spread radius is greater for the glass than the Perspex is recovered.

Result Set	Experimental $\xi$	Numerical $\xi$	Correlation, [4]
I	3.62	4.02 (+14%)	3.55 (-2%)
II	3.31	3.78 (+11%)	3.21 (-3%)

Table 2. Spread radii found experimentally, numerically, and from the correlation of Scheller and Bousfield, [4].

Table 2 shows the different values of the maximum spread radii obtained experimentally, numerically, and from the correlation of Scheller and Bousfield, [4]. Fluent over-predicts the final spread radius by about 14% for the impact on glass and by 11% for the impact on Perspex. For both set of results the correlation proposed by Scheller and Bousfield very closely predicts the maximum spread radius with a maximum relative difference of 3%. Because this correlation and the numerical results were obtained for a Newtonian fluid, this tends to suggest that, in the tested regime, the effect of the non-Newtonian rheology of the blood is minor. Figure 6 shows the droplet height variation as a function of time obtained from the numerical simulation. We

clearly observe two different stages: a steep linear decrease of the droplet height followed by a much smaller one.

In spite of the fact that the value of  $K_d$  in the experiment was found to be greater than 57.7 (see Table 1), the threshold beyond which splashing starts to occur according to Mundo et al. [2], no splashing was apparent in the pictures, a possible consequence of the blood rheology.

## Conclusions

This work is first attempt to simulate the impact of blood droplet on surfaces with the aim of understanding and predicting bloodstain formation. For this work, we used the commercial CFD software Fluent to model the impact dynamics and compared the results with experimental data obtained by releasing blood droplets from a given height and letting them fall on a glass or Perspex surface. The results of the simulations are encouraging as they capture the overall trend of the spread radius evolution and the final spread radius is recovered to within 15%. The simulation is found to over-predict the maximum spread radius. It could be a consequence of the contact angle which is chosen to be the fixed static value when it is well-known that the observable contact angle is a function of the contact-line velocity. Interestingly, the correlation proposed by Scheller and Bousfield gives a very good estimate of the final spread radius in spite of the fact that it is meant for Newtonian fluids. We can deduce that for the parameters used, the non-Newtonian rheology of the blood is of negligible influence. Future work will focus on improving the treatment of the dynamic contact angle on one hand and on considering oblique impacts as those are of paramount importance for forensic scientists.

## Acknowledgments

The authors gratefully acknowledge the support of ESR for this research work and the contribution of the summer interns Estelle Barnett and Bronwyn Smit.

## References

- [1] Brackill, J.U., Kothe, D.B. & Zemach, C., A continuum method for modelling surface tension, *J. Comp. Phys.* **100**, 1992, 335-354.
- [2] Mundo, C., Sommerfeld, M. & Tropea, Droplet-wall collisions: experimental studies of the deformation and breakup process, *Int. J. Multiph. Flow*, **21**, 1995, 151-173.
- [3] Rioboo, R., Tropea, C. & Marengo, M., Outcomes from a drop impact on solid surfaces, *At. Sprays*, **11**, 2001, 155-165.
- [4] Scheller, B.L. & Bousfield, D.W., Newtonian drop impact with a solid surface, *AIChE J.*, **41**, 1995, 1357-1367.
- [5] Yarin, A.L., Drop Impact Dynamics: Splashing, Spreading, Receding, Bouncing, ..., *Annu. Rev. Fluid Mech.*, **38**, 2006, 159-192.
- [6] Yokoi, K., Vadillo, D., Hinch, J & Hutchings, J.I., Numerical study of the influence of the dynamic contact angle on a drop impacting on a dry surface, *Phys. Fluids* **21**, 2009, 072102.